Chapter 11
Hybrid Circuit Breakers with Transient Commutation Current Injection

Z. John Shen, Steven Schmalz, Steven Chen, and Dong Dong

1 Introduction

Hybrid circuit breakers (HCBs) combine the advantages of mechanical and solid-state circuit breakers and offer low conduction losses, high interruption capability, and reasonable response times of several milliseconds. As discussed in other chapters of this book and survey papers such as [1, 2], there are a multitude of HCB topologies, each having distinct advantages and disadvantages but all featuring two parallel current paths: a mechanical path for conducting the load current efficiently under normal conditions and an electronic path to commutate a fault current from the mechanical path under a fault condition and then turn off after the mechanical switch fully opens. In addition, one or more varistors (MOVs) are placed in parallel to clamp the overvoltage surge during the turnoff of the electronic path and to absorb the residual electromagnetic energy. For example, the electronic path can be a passive or active LC resonant circuit in parallel to the mechanical path. When the mechanical switch (MS) opens in response to a circuit fault, the LC circuit would

Z. J. Shen (✉)
Simon Fraser University, Surrey, BC, Canada
e-mail: zjshen@sfu.ca

S. Schmalz
Eaton, Menomonee Falls, WI, USA
e-mail: SteveSchmalz@eaton.com

S. Chen
Eaton, Moon Township, PA, USA
e-mail: StevenZChen@eaton.com

D. Dong
Virginia Polytechnic Institute and State University, Blacksburg, VA, USA
e-mail: dongd@vt.edu

I. C. Kizilyalli et al. (eds.), *Direct Current Fault Protection*, Power Systems,
https://doi.org/10.1007/978-3-031-26572-3_11

generate a resonant current which cancels the mechanical current at certain time instances, subsequently creating zero current crossings in the mechanical path to aid the opening of the mechanical contacts. A true arcless HCB concept through the use of a load commutation switch (LCS) in series with the mechanical switch was developed by ABB [3–7]. The LCS, made of semiconductor switches with a much lower-voltage rating than the HCB, forces the fault current to commutate from the mechanical to the electronic path when being turned off. The mechanical contacts can therefore open under a true zero current condition without any arcing. One major drawback of the LCS approach, however, is the additional conduction power losses on the LCS, which still has on-state resistance many times that of the mechanical contacts even with a large number of lower-voltage power devices being used in parallel. LCS power losses will become an even bigger challenge with a significant penalty in size and weight as the HCB current rating increases and thus needs to be addressed with innovative solutions.

A new HCB architecture was recently proposed which uses a switching-mode transient commutation current injector (TCCI) instead of the series LCS approach to commutate the fault current from the mechanical to the electronic branch and realize arcless breaker operation [8, 9]. The TCCI circuit remains in a standby mode with near-zero power loss under normal conditions but can rapidly generate a pulse current dynamically matching the fault current and therefore facilitate current commutation from the mechanical to the electronic path. It completely eliminates the conduction power loss associated with the LCS and delivers an ultra-high transmission efficiency. A relatively low-power TCCI-based HCB prototype demonstrated a total active response time of 310 μs and a peak interrupted fault current of 89 A at a DC voltage of 400 V [9].

In this chapter, we will report the development of a 6-kV/200-A TCCI-based HCB designed for medium-voltage DC (MVDC) applications, funded by the US Department of Energy ARPA-E BREAKERS Program [10]. MVDC holds the promise of addressing limitations faced by legacy AC systems including (1) better utilization of existing infrastructure, (2) improved network stability and simplified management of power flow, (3) lower transmission/distribution losses, and (4) easier integration with renewable energy sources. A key to realizing MVDC systems is meeting the requirement for overcurrent fault protection. The development of TCCI-HCB for MVDC power ratings presents unique technical challenges and design considerations in terms of subsystem design, system integration and packaging, control and communication, and dielectric isolation. We will discuss these design issues after a brief review of the basic TCCI-HCB concept.

2 Basic Concept

Figure 11.1 conceptually depicts the circuit topology and switching waveforms of the total load current i_L, mechanical branch current i_M, and electronic branch current i_E during the interruption operation of the HCB in response to a fault condition.

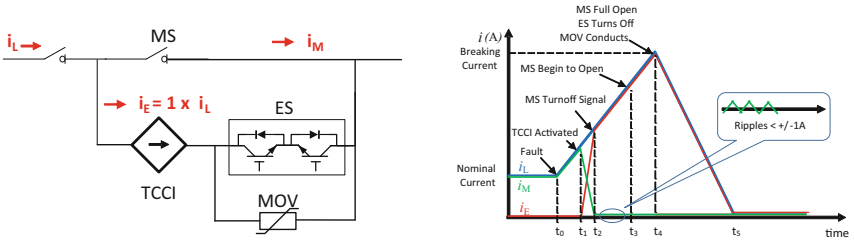

Fig. 11.1 Notional circuit topology and switching waveforms of an HCB with transient commutation current injector (TCCI) [9]

A switched-mode TCCI circuit, shown as a current-controlled current source in Fig. 11.1, is placed in the electronic path. It remains inactive with near-zero power loss during normal operation until t_0 when a short-circuit fault occurs. At t_1, the overcurrent condition is detected. At this point, the TCCI will immediately inject a pulse current i_E from its pre-charged capacitors and dynamically track the fault current with high precision and force the fault current to commutate from the mechanical to the electronic path at t_2. The current through the mechanical branch will remain as a small high-frequency AC ripple current until the mechanical switch (also referred to as high-speed vacuum switch or vacuum disconnect switch later in this chapter) opens at t_3. The small AC ripple current results from the control errors of the TCCI and has the same switching frequency in the range of 100–200 kHz as the TCCI. The mechanical vacuum switch receives a turnoff signal at t_2 and generates a gap between the contactors at t_3 after a short delay without arcing under the near-zero current condition, leaving the electronic branch to carry the entire fault current during t_2 to t_4. At t_4, the mechanical vacuum switch provides a sufficiently wide gap to support the rated voltage, and the electronic switch (ES or referred to as power electronic interrupter (PEI) later in this chapter) turns off, leaving the metal oxide varistor (MOV) to absorb the residual electromagnetic energy during t_4 to t_5.

3 HCB Subsystems

The TCCI-HCB is comprised of several key subsystems, including transient commutation current injector (TCCI), high-speed vacuum switch (HSVS), power electronic interrupter (PEI), and auxiliary power supplies with high-voltage isolation capability. This section discusses the operation principles and design considerations of those subsystems in detail.

3.1 *Transient Commutation Current Injector (TCCI)*

TCCI is the most critical subsystem in the new HCB architecture. The crucial performance target of the TCCI design is its capability of dynamically tracking the fault current within a short delay (<30 μs) and with a high precision (<5%). The TCCI is a switched-mode power electronic circuit, similar to the design of high-current high-precision pulse power sources used for controlling the magnetic fields in linear accelerators [11, 12]. These current sources can quickly generate a pulse current of several kA with extremely small tracking errors (current ripples) of 10–100 ppm (0.001–0.01%) from a pre-charged capacitor bank. It is worth noting that our TCCI needs to track a time-varying fault current instead of a constant "flattop" reference current in these pulse current sources. This challenge can be addressed by operating the TCCI converter at a high PWM frequency for superior dynamic response. On the other hand, our TCCI only needs to operate for hundreds of microsecond instead of hundreds of millisecond as in these prior-art pulse current sources and thus needs a much smaller energy storage capacitor (typically hundreds of microfarad) and power and cooling components with significantly reduced power ratings for this unique "single-shot" pulse mode operation. The TCCI design should be fairly compact and inexpensive.

A simplified bidirectional TCCI topology is proposed in this work as shown in Fig. 11.2, along with other key subsystems of the HCB, such as the vacuum interrupter (VI) and power electronic interrupter (PEI). A 3D rendering of the TCCI is also shown in Fig. 11.2 with the key components clearly labeled. The TCCI is comprised of three parts: a simple buck converter made of IGBT Q_1, freewheeling diode D_1, and filter inductor L_1; a bidirectional current-steering bridge made of four

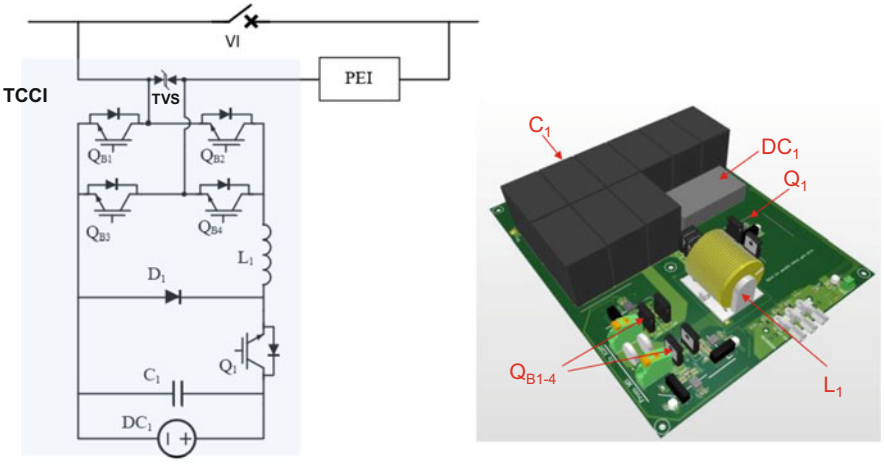

Fig. 11.2 Simplified bidirectional TCCI circuit diagram along with the vacuum interrupter (VI) and power electronic interrupter (PEI) subsystems of the HCB. A TCCI physical design is also shown

IGBTs, Q_{B1}, Q_{B2}, Q_{B3}, and Q_{B4}, and a transient voltage suppresser (TVS); and a capacitor bank C_1 along with its charging power supply DC_1. Depending on the direction of the current in the electronic path, either Q_{B1}/Q_{B4} or Q_{B2}/Q_{B3} is in the on-state to inject a countercurrent to VI through PEI. The TVS is used to prevent undesirable transient overvoltage across the output terminals of the bridge circuit. The basic function of the buck converter is to generate a transient countercurrent to precisely cancel the mechanical branch current by discharging the pre-charged capacitors C_1 in a well-regulated manner. Once an overcurrent condition (e.g., 2× of the nominal current) is detected, Q_1 turns on for a certain period of time to provide an initial pulse current injection within a few tens of microsecond to quickly commutate the mechanical branch current to the electronic branch. During the next 200–500 μs, Q_1 turns on and off in a PWM mode to regulate the TCCI output current, so it closely matches the continuously increasing fault current. The pre-charged C_1 serves as the input energy source for the buck converter. During this phase of operation, the main objective of the TCCI is to track the fault current with a high precision and ensure only a small AC ripple current through the mechanical VI so it can open under a near-zero current condition. After the VI is fully opened, Q_1 turns off, leaving the total fault current flow through D_1, L_1, and Q_{B1}/Q_{B4} or Q_{B2}/Q_{B3} without active control (freewheeling current). PEI is the main static switch in the electronic path, which turns off after VI completely opens as will be discussed later in this chapter. A dual-band hysteretic control method for the TCCI is adopted, which offers fast dynamic response and excellent stability. By carefully selecting the two bandwidths of the dual-band hysteretic PWM controller, the high- and low-voltage phases will work in concert as the coarse (quick) and fine tuners for the high-precision current source. Note that the TCCI is on standby with near-zero power loss during normal operation.

The TCCI design needs to be optimized based on the voltage and current ratings as well as the timing requirement (i.e., how fast the mechanical VI can fully open), including the selection and sizing of the key components (energy storage capacitors, inductor, power transistors, and current sensors). The TCCI essentially discharges the pre-charged capacitors C_1 in a well-controlled manner to generate the required transient commutation current pulse. It is important to select the right size and voltage level of C_1 to ensure sufficient charge storage while avoiding cost and size penalty. Since the TCCI only needs to be activated for a very short time period (typically hundreds of microsecond) when the HCB needs to turn off, it is C_1 that supplies the high pulsed current, while a small isolated DC power supply DC_1 (only rated at a few watts) only serves to pre-charge C_1 when the circuit is under normal operation. In the 6-kV/200-A HCB design case, C_1 is in the range of several hundreds of microfarad with an initial charging voltage of 500–550 V. Film capacitors can be used for this purpose as shown in Fig. 11.2. The value of L_1 is determined by the trade-off between the requirement of the initial fast rise of the TCCI injection current and the requirement of a small AC ripple of the TCCI current after the initial rise. The *di*/*dt* of the TCCI current needs to be 5 ~ 20 times greater than that of the fault current (typically 1–2 A/μs) so the TCCI can effectively commutate the fault current from the mechanical to the electronic path. On the other

hand, the AC ripples on the TCCI current after the initial fast rise needs to be within 5% of the total current so the mechanical contacts can separate without arcing. In the 6-kV/200-A HCB design case, L_1 is in the range of 10–30 μH. Furthermore, 1200-V IGBTs and FRDs are selected for Q_1 and D_1, respectively. 600-V IGBTs are selected for bridge transistors Q_{B1}, Q_{B2}, Q_{B3}, and Q_{B4}. During the TCCI operation, Q_1 switches at a PWM frequency of 100–200 kHz but only for a small number of cycles, similar to pulse power applications; thus, the relatively high switching loss of the IGBTs can be tolerated. The concern here is more associated with reducing the voltage drop across the IGBTs at a very high fault current up to 1000 A.

3.2 High-Speed Vacuum Switch (HSVS)

A second key element in the HCB architecture is the high-speed vacuum switch (HSVS), which serves as the primary conduction path under normal operation of delivering power to the load. Design of the HSVS incorporates a fast actuator, damping and latching mechanisms, and an optimized vacuum interrupter. It is essential to effectively combine all these elements to realize a mechanical switch capable of achieving an interruption time of less than 0.5 ms.

3.2.1 Fast Actuator

High speed and fast response are the primary requirement for this type of mechanical switch in the MVDC hybrid circuit breaker application. In conventional mechanical circuit breakers for AC circuit protection, a typical response time is about 50 ms from the moment of initiating a trip command to actual breaking of the circuit. In this specific design, the required response time (<0.5 ms) is about 1/100th that of a typical mechanical circuit breaker. Contact gaps of MV vacuum interrupters are generally between 2 and 12 mm, depending on voltage ratings and actual applications [13]. For this 6-kV/200-A HCB design, a high-speed vacuum switch (HSVS) is developed with a DC voltage and current rating of 6 kV and 200 A, a contact gap of 6 mm, and a contact moving mass of about 0.5 kg. There is a significant difference in the estimated kinetic energy needed to drive a conventional vacuum switch versus an HSVS because of the different response time requirements. A conventional switch or breaker with a similar moving mass would need a kinetic energy of 0.5–1.0 J to reach an average opening speed of 1–1.5 m/s across a 6-mm gap to interrupt the AC current with mechanical efficiencies fully considered. The new HSVS design, on the other hand, needs a kinetic energy of approximately 9 J to achieve an average speed as high as 6 m/s to meet the specified response time. Since the response times are significantly different between the two (50 and 0.5 ms), the times to disburse the energy are very different too, which dictates the power of actuation. The instantaneous power needed to drive the contact in a conventional design is approximately 150 W. For the HSVS, the power needed may

exceed 18,000 W in order to achieve the required response time for successful fault current interrupting operation.

The large power requirement of the new HSVS determines the type of actuation technology that needs to be used. Actuator mechanisms widely used for conventional switches or circuit breakers, such as springs or solenoids, are no longer practical for the HSVS. Other actuation means need to be explored considering size, weight, cost, and capability of instant power factors. As alternative methods, piezoelectric actuators (material force) and Thomson coils (field force) demonstrate their potential to provide quick acceleration for a movable contact. Piezoelectric actuators have advantages in terms of precision, speed, high force, and durability but can only deliver very small displacement. It is difficult for a piezoelectric actuator to realize more than 1 mm of contact travel even with sizable and sophisticated displacement amplifiers [14]. For the HSVS design in this work, we choose not to adopt piezoelectric actuators after detailed analysis, especially with the consideration of design scalability to higher voltage and current ratings. Thomson coil actuators, an application of Faraday's law of induction, can also produce enough force to move the contacts quickly with larger travel distances. They are particularly effective for vacuum interrupter contacts that normally need to a gap of several millimeters for high dielectric withstanding ability. In a typical form factor volume for a modern MV vacuum switch or circuit breaker, a Thomson coil actuator can produce forces of tens or hundreds of thousands of Newtons, which is impossible for conventional mechanisms to match. Figure 11.3 conceptually shows the anatomy of the new HSVS in this work. The vacuum interrupter (VI) is placed on the top which is mechanically linked to a primary Thomson coil actuator by an insulated drive link rod. The HSVS subsystem also includes an over-toggle damping mechanism and a shock absorber.

There are many factors that must be carefully considered to properly design a Thomson coil actuator. The drive current characteristics (including stored energy requirements), coil impedance, geometry and metallurgy of the moving plate, and overall mechanical configuration must be determined. An assortment of interdependent parameters influences these characteristics and dictates what is and what is not achievable. It can be overwhelming at first look, but the key is to clearly define the required performance of the actuator, which may include efficiency, size, physical constraints for integration, and manufacturing considerations. As in most endeavors, knowing what matters most will lead to an optimized design for the intended purpose [15]. Actually, having so many customizable variables in Thomson coil design is an advantage and provides opportunity for scalability.

Damping Mechanism

A defined open-contact position is always required, even in the case of an HSVS designed for current commutating operation of the HCB. While its initial contact gap of 1–2 mm is critical for successful current commutation and transient voltage withstanding, a wider and settled open-contact gap, 6 mm in this case, is also

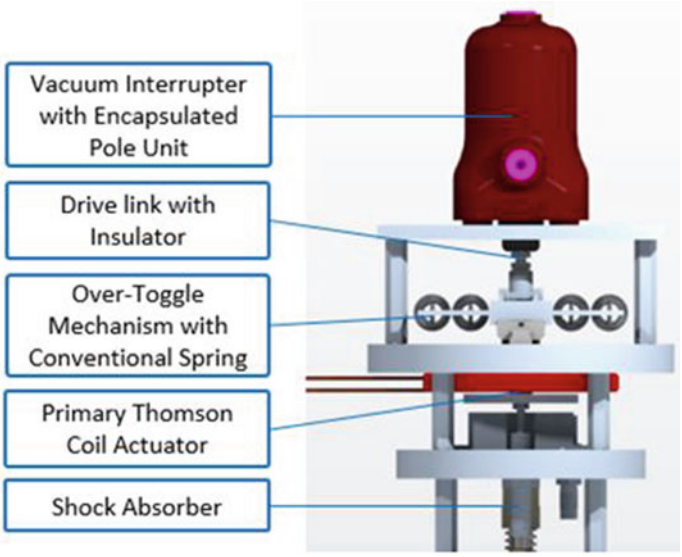

Fig. 11.3 High-speed vacuum switch (HSVS) anatomy

needed. The larger gap is needed to safely withstand, in some conditions, prolonged voltage stresses or occasional voltage surges from the power system in which it is installed, especially when the circuit breaker is in a "hot" standby condition where the disconnector for the line remains closed. While opening speed is the key for achieving the desired performance of current interruption, a controlled deceleration of the moving contact cannot be neglected. The residual kinetic energy stored in the moving mass of the moving contact can be significant, reaching more than ten times that of a conventional vacuum switch. If there is no means provided to properly absorb the residual kinetic energy, the contacts can bounce back, resulting in reduced contact gap during the transient phase of current interruption or commutation that may lead to voltage breakdown. Otherwise, contact overtravel could also occur, which will overstress the bellows of the vacuum interrupter resulting in reduced mechanical life.

Damping can be an efficient method to deal with the residual kinetic energy and can be realized by using commercially available shock absorbers [16]. Although the wide variety of available options may satisfy the specific performance requirement, cost, size, and reliability have to be considered in final selection. For this new design, commercial-type of shock absorbers are used as a quick and feasible solution. Proper damping can sufficiently absorb the energy, but in addition, a purposefully customized damping profile can control contact gap establishment to positively influence events including current commutation, arc interruption, and dielectric strength recovery which happen at different stages in the contact parting process. Contact material, contact configuration, and the targeted application must also be factored into the sequence.

Latching Mechanism

The movable contact of the new HSVS needs to be securely latched in two stable positions, closed and open, similar to all conventional vacuum switches or circuit breakers. The latching in conventional switches or circuit breakers is commonly made by mechanical mechanisms with multiple parts or magnetic mechanisms. If there is anything special for the HSVS, it is with respect to its requirement for fast response. The impact of the latching mechanism due to faster response time must be minimized and could be affected by added mass, rotating joints, or demagnetizing time. To latch the contact open, faster opening speed leaves less time for a latching mechanism to operate. In a conventional switch or circuit breaker, the time for the latch to operate is on the order of tens of milliseconds. For the new designed HSVS, the latching operation must be completed within 0.5 ms. The challenges mandate a simplified latching mechanism that contains less parts and joints, although more complex alternative solutions may still exist. The final implementation employed an over-toggle latching mechanism design for the HSVS, which is able to latch the moving contact in both closed and open positions.

Vacuum Interrupter

A mechanical switch for an MVDC hybrid circuit breaker application must be capable of (a) switching off the circuit quickly to assist the completion of fault current commutation and (b) withstanding the high rate of rise of interruption recovery voltages generated by the power electronic interrupter during its turnoff operation, especially when very fast response time is required. The recovery voltage rate of rise can be more than 5 kV/μs, even greater than that of the standard lightning impulse voltage, which is about 3.5 kV/μs [17]. These required capabilities make vacuum interrupters stand out from all other mature switch technologies in medium-voltage applications. The advantage is rooted in the vacuum interrupter's superior dielectric strength and its quick recovery from the transient state during current switching or interruption [13] (see Table 11.1). The advantage makes vacuum interrupters particularly suitable for MV HCB applications where fast response time is demanded because the high dielectric strength allows for a smaller contact gap and the shorter distance reduces travel time. In addition, the quick recovery of dielectric strength makes current interruption faster which reduces the time of current commutation. Finally, short-contact travel distances require less energy to drive the actuator which reduces the size of actuation mechanism.

Table 11.1 Dielectric strength of common insulation materials used in medium-voltage rated equipment

Dielectric strength (kV/mm) (in general good condition)	
Vacuum	~20
Mineral oil	~15
SF6	~10
Dry air	~3

Fig. 11.4 Vacuum interrupter (VI) employed in the HSVS

Figure 11.4 shows the vacuum interrupter used in the HSVS. It measures about 50 mm in diameter and 75 mm in length. During the current interruption operation of the HCB, the current commutation is completed before the vacuum contacts separate. At the same time, it is subject to peak transient interruption recovery voltage generated by the power electronic interrupter of 12 kV with a rate of rise greater than 5 kV/μs. The stable open gap is set to 6 mm to reliably withstand 20 kV for 1 min, in case extended voltage withstanding is needed.

Figure 11.5 illustrates the anatomy of a typical vacuum interrupter. Medium-voltage vacuum interrupter technology has been well developed over more than 60 years and is used in many applications, from load switching to generator protection. There are many variables which can be managed in a design, such as contact material, contact structure, shield profiles, contact position, or electrode lengths, among others, to address the needs of a particular application. These needs may include dielectric performance, interruption capacity, energy efficiency, etc.

Though it is mature in technology for conventional designs and applications, the HSVS for HCB application poses a new challenge to the vacuum interrupter – the mechanical life of its bellows under repeated high-speed impacts. In a vacuum interrupter, the bellows, which are usually formed from thin stainless steel sheets, are subjected to impulse force and motion as the contact is made to open and close with different acceleration rates, speeds, and often sudden stops. With continuous improvement over the decades, the mechanical life of the bellows in a conventional circuit breaker's vacuum interrupter is in the range of 10,000–30,000 operations. For contactors' vacuum interrupters, the bellows' mechanical life may exceed 1×10^6 operations, where the contact gap can be smaller and contact moving speed can be slower. In all these, the contacts' speeds are normally within 2 m/s.

The HSVS performance specifications stated above are not from calculations or simulations. Rather, they are instead from real tests with real circuit breakers and switches. They are accumulated general results. There may be no practical tool to allow plugging in parameters to predict reputable mechanical life of VI bellows. Nevertheless, a large variety of bellows are commercially available designed to

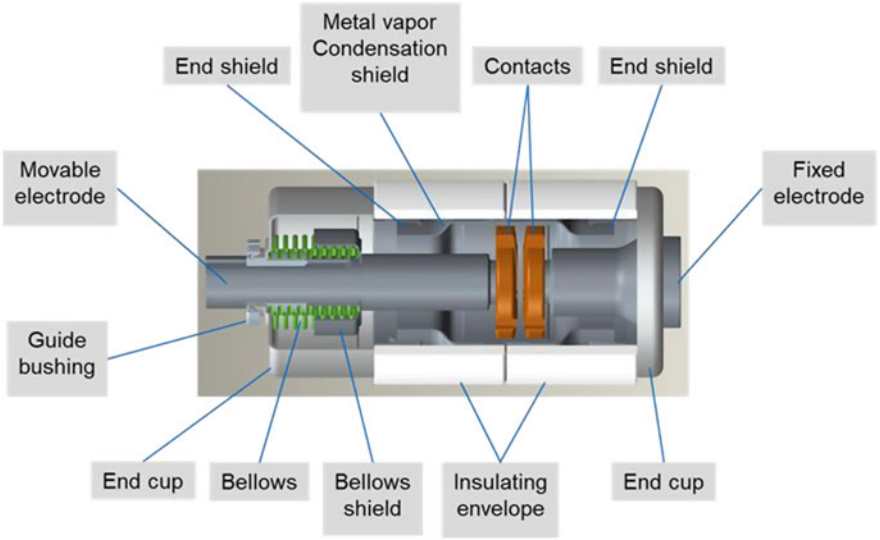

Fig. 11.5 Vacuum interrupter (VI) anatomy

many different service conditions in vacuum interrupter applications with accumulated knowledge and experiences, especially from reputable manufacturers. Although the conditions of the vacuum interrupter used in the newly designed HSVS are considered unusual at this time, to select its bellows from the commercially available options is a practical first step. Initial experiments indicated that its mechanical life has a good chance to be in range of that for conventional vacuum circuit breakers. Careful future optimization of the actuation and damping will only improve its longevity.

3.3 Power Electronic Interrupter (PEI)

The power electronic interrupter (PEI) is the third key subsystem in the HCB and functions essentially as a high-power solid-state switch. It is responsible for interrupting the fault-current and ultimately driving it to zero in a very short period after the VI completely opens. This is enabled by creating a transient voltage across PEI higher than the DC source voltage. Therefore, the PEI in the HCB acts very similar to a solid-state circuit breaker (SSCB), which needs power semiconductor devices and energy absorption components like MOV. The key difference between PEI in HCB and SSCB is that the PEI only needs to carry the fault current for a short time period like a pulse current. This requires the devices in PEI with a high pulse current capability and a large thermal capacitance. PEI can be designed with power semiconductor devices, such as IGBT, IGCT, or SiC MOSFETs. Among

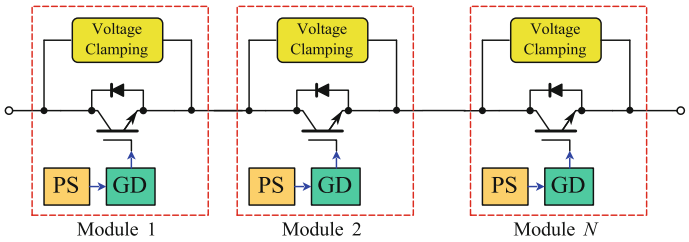

Fig. 11.6 Modular PEI with distributed voltage clamping circuit

them, IGBT presents more design flexibility and benefits in PEI as it can handle high *di/dt* than IGCT and also has a high pulse current ratio due to its large chip size than existing SiC MOSFETs.

As PEI needs to sustain a higher voltage than the DC bus voltage during the current breaking transient, MV IGBTs of 3.3 kV or higher ratings can be considered. To reach even higher blocking voltage than that of a single MV device, series connection of IGBTs can be considered, and the main challenge is the voltage sharing [18, 19]. Therefore, the modular structure as shown in Fig. 11.6 has been adopted in most PEI topologies [20]. For instances, the Zhangbei 500-kV HVDC HCB uses 320 series modules to realize the required blocking voltage requirement [21]. The distributed voltage clamping circuit paralleled with low-voltage device could be regarded as one module, whose maximum voltage is thereby limited and balanced by the voltage clamping circuit. Besides the low cost and high flexibility, another advantage of this modular approach is that the cascading damage can be avoided even when one of the series modules is damaged.

Since the modular structure can handle high clamping voltages, the challenge is to achieve conduction and safe interruption of the fault current. High peak current capability and high transient thermal capacitance are the two key parameters used to select the power devices. The peak current capability is mostly associated with the device material and structure, while the transient thermal capacitance is mostly related to the physical size of the device and the package.

Voltage clamping circuit can help suppress the overvoltage across the device and absorb the energy stored in line inductor. Various voltage clamping components have been discussed in [22, 23], including the metal oxide varistor (MOV), transient voltage suppression (TVS) diode, resistor-capacitor (RC) snubber, etc. The design of voltage clamping circuit is typically driven by the peak clamping voltage, the leakage current at nominal voltage, and the total absorption energy. MOV is a nonlinear resistor with its resistance value as a function of the applied voltage [24]. When a low voltage is applied, it has a very high resistance, whereas it has the lowest resistance with the clamping voltage applied. Besides, there is a steep front effect to affect the peak voltage, which is proportional to *di/dt* [25].

To reduce the *dv/dt* and *di/dt* impact to the device and the gate-driver circuit, a snubber circuit is usually needed in PEI. Figure 11.7 shows a typical RC-based

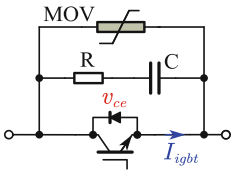

Fig. 11.7 MOV paralleled with RC snubber

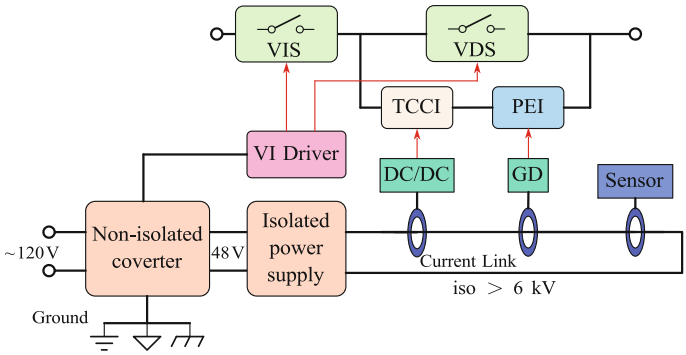

Fig. 11.8 Auxiliary power supply architecture for the HCB system

snubber circuit that is paralleled with the MOV. The RC snubber could also help lower the turnoff power loss and limit MOV voltage overshoot [20].

In the whole system, the auxiliary power supply needs to deliver the power for all electronic and sensing components in HCB. The drive circuit for the Thomson coil of the vacuum disconnect switch (VDS) (a.k.a. the high-speed vacuum switch) and VIS does not need isolation, because the insulation layer is inserted between the coil and the VI [15, 26]. However, an isolated power supply with enough insulation capability is necessary to drive the TCCI, PEI, and some sensors as shown in Fig. 11.8. The insulation capability should be at least higher than the maximum voltage seen by the system, i.e., the clamping voltage. This high-insulation capability makes the auxiliary power supply special than other applications. There are many auxiliary power supply solutions that offer high-insulation capability. But considering the different locations and power rating of multiple loads, a current-link single-turn transformer-based power supply is considered in this work [27].

As shown in Fig. 11.9, the primary circuit can provide a constant sinusoidal current i_p, while the secondary side uses a diode bridge and a boost converter to regulate the output voltage. By changing the turn number of secondary winding, the output power rating is changed accordingly. Electrical insulation is provided by the single-turn transformer. Within the PEI unit, due to the modular structure, the gate-driver power supply for IGBT in each module should be isolated with each other. Although the gate-driver voltage potential difference between the first module and last module will be the total clamping voltage, the voltage potential difference between two nearby modules will not exceed the clamping voltage of selected MOV. Therefore, a cascade power supply architecture can be adopted inside PEI to reduce

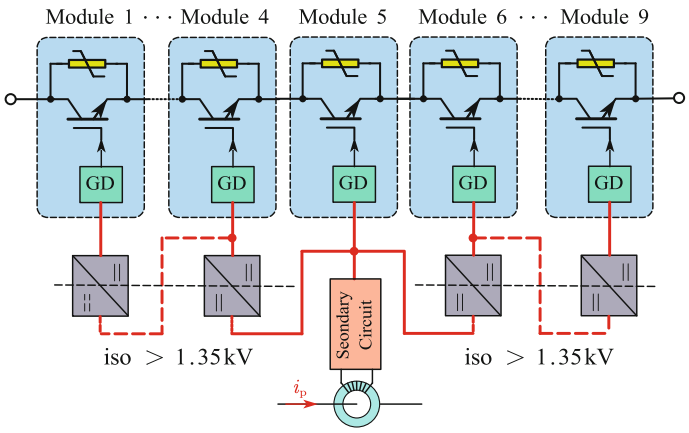

Fig. 11.9 Cascaded gate-driver power supplies used in PEI

the isolation voltage requirement for the small gate-driver power supply. As shown in Fig. 11.8, the output of secondary circuit is connected to the middle module, and then the power is delivered to series modules one by one. In this way, the commercial compact DC/DC power supply used for MV IGBT gate driver is sufficient to meet this isolation voltage requirement.

The interruption time of the HCB is predominantly limited by the opening speed of the mechanical contacts, which is greatly slower than that of SSCB. Gap distance and contactor opening speed of the VDS are in the range of tens to hundreds of microsecond per millimeter gap. Only after enough dielectric strength has been established across contacts of the VDS will the PEI be allowed to be turned off as shown in Fig. 11.1 (t_4). Otherwise, the arcing of VDS will occur to commutate the current back to the VDS branch and cause the failure of HCB. A long waiting time for PEI leads to a very large peak current and a long total HCB interrupting time.

In order to reduce the waiting time for the PEI, a staged turnoff strategy is introduced in [28] to make full use of the gap distance curve. Since the PEI consists of series identical modules, they could be turned off sequentially to create a staged clamping voltage waveform as shown in Fig. 11.10. The coordination of the PEI turnoff sequence and opening of the VDS contacts is very important to make sure that arcing will not occur. It can be seen that the peak fault current, total absorption energy, and clearing time will be reduced after applying this staged turnoff strategy.

4 System Control and Integration

Key to the implementation of the hybrid circuit breaker is the coordination and control of all the subsystems described above. As described earlier in the principle

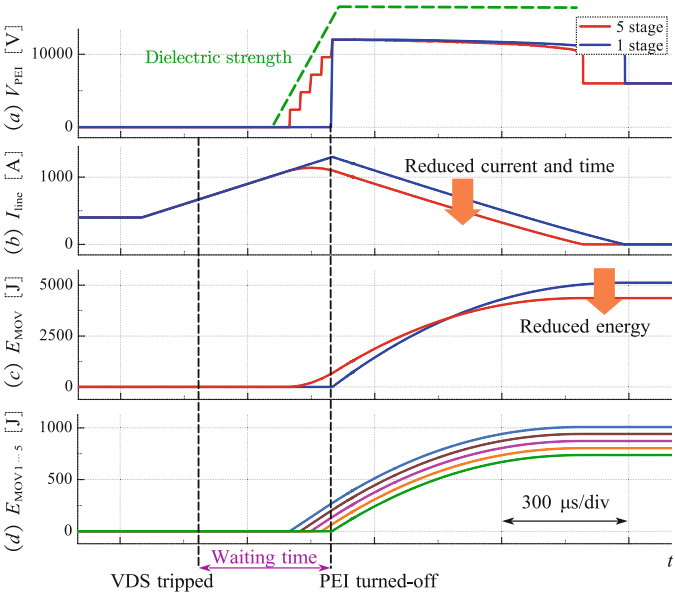

Fig. 11.10 Comparison between single-stage and five-stage turnoff schemes

of operation for the circuit breaker's interruption sequence, each component must operate precisely in the prescribed order to successfully interrupt the current flow. As a designer, one must weigh the options when it comes to implementation of a compact, cost-effective, and robust control scheme. Both centralized and distributed control architectures were considered for this hybrid design. Given the fact that the circuit breaker is primarily a self-enclosed system with the subsystems in close proximity, a distributed architecture provides no particular advantage and would likely add complexity from both hardware and software perspectives. Therefore, a centralized control architecture was employed as it offered the most efficient approach to achieve the precise timing required and avoid potential latency challenges with distributed control methods while minimizing electronic hardware in each requisite subsystem. Figure 11.11 conceptually depicts the hardware control architecture of the HCB system in this work.

By nature, circuit breakers designed for medium voltage have unique requirements when it comes to providing dielectric isolation between the live switching components and the grounded chassis. The necessary circuitry to sense and detect overcurrent faults and control the breaker operation (i.e., trip, reclosure, and nominal switching) is referred to as the "trip unit" and is typically implemented in hardware on a printed circuit board employing a microprocessor in modern circuit breakers. The need to interface with the various components of the HCB (TCCI, PEI, and actuators for the vacuum interrupters), which may be electrically connected and referenced to the medium-voltage potential, presents significant

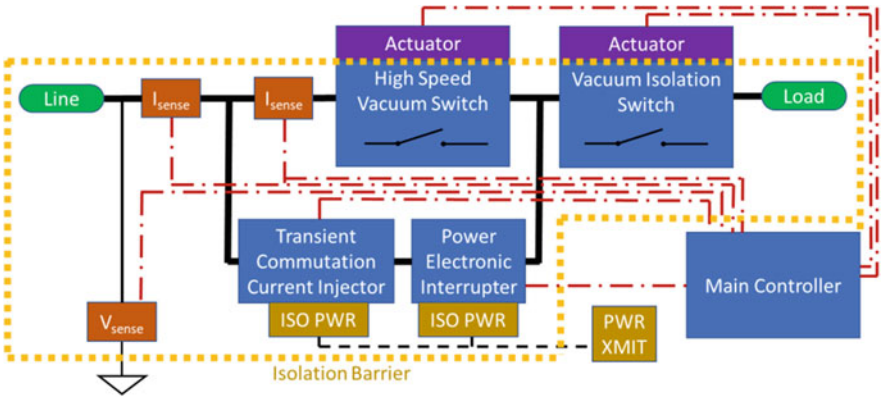

Fig. 11.11 Hybrid circuit breaker hardware control architecture

challenges in trip unit design. The trip unit controller must derive its power, convey command signals, and monitor sensor inputs while maintaining dielectric isolation from the live components. This is fundamental, due not only to the low-voltage nature of integrated circuitry but also to assure safety of the switchgear overall. Industry standards require clearly defined boundaries between ground-referenced components and live elements such that breakdown (i.e., flashover) does not occur and all control elements remain isolated under all circumstances. This includes meeting extreme transient requirements including short-term voltage withstand and basic impulse-level capability (i.e., lightning strike) which can exceed 100 kV depending on breaker rating. Not surprisingly, isolation dictates much of how a circuit breaker's control is implemented.

The means to provide isolated power for the TCCI and PEI power electronic subsystems, as well as sensors, were described in the previous section. In this HCB design, power for the main controller is derived from a dedicated 120-VAC auxiliary control power circuit, which is independent of the medium-voltage mains. While in some low-voltage systems derivation of control power from the mains is possible, it is generally not practical for MV switchgear. Other means of providing control power could also be considered, including lower-voltage DC (24 or 48 V) supplies, but typically they all employ a dedicated source separate from the mains.

Beyond powering the main controller and subsystems is the ability to communicate control signals between these components while retaining MV isolation. Fiber optics are typically employed in MV equipment to meet this requirement. Plastic fiber cables are relatively low cost and provide high dielectric isolation across even short linear lengths if dirt and contamination on the cable surfaces can be environmentally mitigated. Fiber-optic cabling is also not affected by electromagnetic interference (EMI), which is also essential in MV applications where the field intensities can be extreme. Discrete and serial digital data and command signals can thereby be optically exchanged between the controller and MV-referenced components in the breaker. Magnetically coupled approaches could

also be considered for transmission of both power and data across an electrically isolated barrier. However, depending on the level of isolation needed, implementation of magnetic-based isolation techniques may present significant trade-offs for more extreme applications.

Sensing of current and voltage is particularly challenging for MVDC circuit breakers. AC breakers generally utilize current and potential transformers (CT/PT) to monitor real-time electrical parameters during operation. Unfortunately, neither is capable of measuring DC. Other DC-compatible sensors that were capable of providing isolation needed to be employed in the HCB. Current sensing bandwidth requirements of the TCCI posed the most challenging aspect of the control and drove the decision to utilize noncontact Hall effect current sensing. The analog sensor output signals are provided directly to the central controller rather than a digitized serial data stream to minimize latency in signal processing. This approach does present challenges with EMI and retaining adequate levels dielectric isolation, but at the targeted voltage and current ratings for our prototype, these were manageable.

However, as breaker voltage and current ratings scale upward, a designer must be cognizant of the limitations in state-of-the-art sensing technologies. Commercial off-the-shelf sensors are generally not designed for the rigors of the medium-voltage environment where partial discharge phenomena can compromise component life. Furthermore, in circuit breaker applications, sensors must be able to be subjected to extreme transients without lasting degradation to their performance. Specific design considerations must be made when applying Hall effect, flux-gate, and magneto-resistive current sensing methods to address these extremes. Furthermore, as breaker ratings scale up, so too do the sensing dynamic range requirements, which often leads to compromises in precision and bandwidth. All these aspects must be considered in the control design, and more advancements in current sensing will likely be needed to meet the needs of future high-power MVDC systems.

5 Experimental Results

Experimental validation of the TCCI-based hybrid circuit breaker took an incremental approach, with each subsystem tested individually as a standalone device. This allowed each project development team to work independently at first and to progressively evolve the essential functionality of the subsystem designs prior to completion of the overall control architecture and without impact on other teams. This typically involved functional emulation of other subsystems to validate the basic system-level operation in tests at reduced voltage and current levels. For example, early versions of the TCCI used a commercial off-the-shelf vacuum relay and single-stage IGBT switch to mimic the behavior of the high-speed vacuum switch and power electronic interrupter, respectively, while it was still in development. After first exploring design alternatives in simulation and basic breadboards, multiple iterations of hardware for each subsystem were progressively built and tested, as described in previous sections. Eventually, prototype assemblies

rated for the full 6-kV voltage target were prepared and ready for mating in system integration testing and debugging.

Integration started in the Illinois Institute of Technology (IIT) with the TCCI hardware platform as the base element. This platform was capable of conducting circuit interruption tests at source voltages up to 1 kV and peak currents up to 200 A by discharging a low-voltage capacitor bank to simulate a bolted fault condition. The first step in integration was to replace IIT's original controller, which was only configured to operate the scaled down emulated components, with a full-functional controller with interfaces for the full-scale assemblies. Once the control hardware and software portability were validated, the next step was replacing each emulated component in turn with the fully rated subsystem. These tests validated additional control circuitry and software on the main controller to operate the actual multistage PEI and HSVS actuators with proper timing of the interruption sequence. It was during these tests that some anomalous behavior of the TCCI was observed, stemming from the fact that the single-stage emulated PEI that was used in its development exhibited a much lower on-state voltage drop than the fully scaled PEI design. The higher-voltage drop made it more difficult for the TCCI to commutate higher peak fault current levels. Improvements to remedy the problem have been identified and will be employed in future prototypes. Regardless, the TCCI functioned more than adequately enough to validate the HCB's operating principle at the peak interruption current-level goals for the initial testing milestone of 200-A peak.

The successful rounds of testing at IIT paved the way for the final test series at the Virginia Tech CPES lab at the target full 6-kV rated voltage for the HCB and at higher peak interruption current levels. The final hardware test configuration included the main controller board (with further upgraded software), the nine-stage PEI, the TCCI 1.0 power block, and a new HSVS assembly with integrated high- and low-speed actuators. The mechanical switch assembly also incorporated the vacuum isolation switch (VIS) encapsulated pole unit with actuator, although it was not operated and remained closed throughout the interruption testing, as its operation was not fundamental to the interruption process. In order to also validate the complete HCB packaging concept as much as possible, the electronic PCBs were mounted to a vertical panel adjacent to the HSVS/VIS assembly in nearly identical position as that envisioned for the final HCB prototype. The lab test setup is illustrated in Fig. 11.12.

As before, overcurrent faults were facilitated via discharge of a capacitor bank charged to a predetermined bus voltage, since no continuous MVDC sources readily exist for this type of testing. We utilized CPES's medium-voltage test bay which is equipped with a 2.3-mF capacitor bank rated to 10-kV DC with a charging power supply. Two series configured 6.5-kV IGBT modules served as a test control and emergency interrupt switch, to both initiate the test by applying the 6-kV bus to the closed breaker assembly and also disconnect power if the breaker failed to open within the prescribed timing. Various combinations of series inductance and resistance were used to limit fault current peak and rise time in the form of fixed

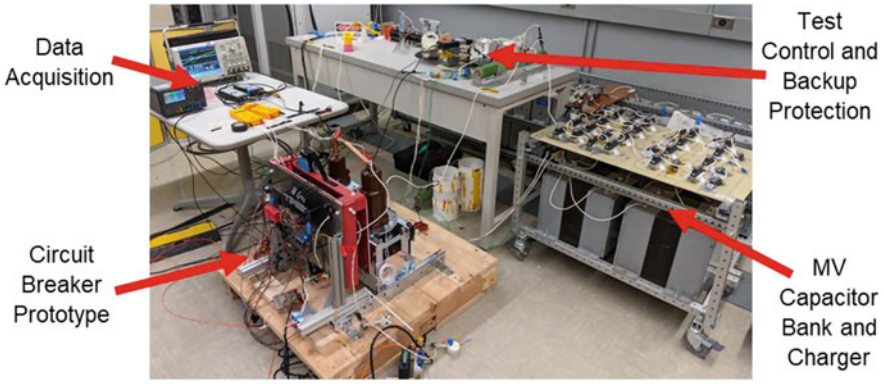

Fig. 11.12 6-kV capacitive discharge interruption testing in lab

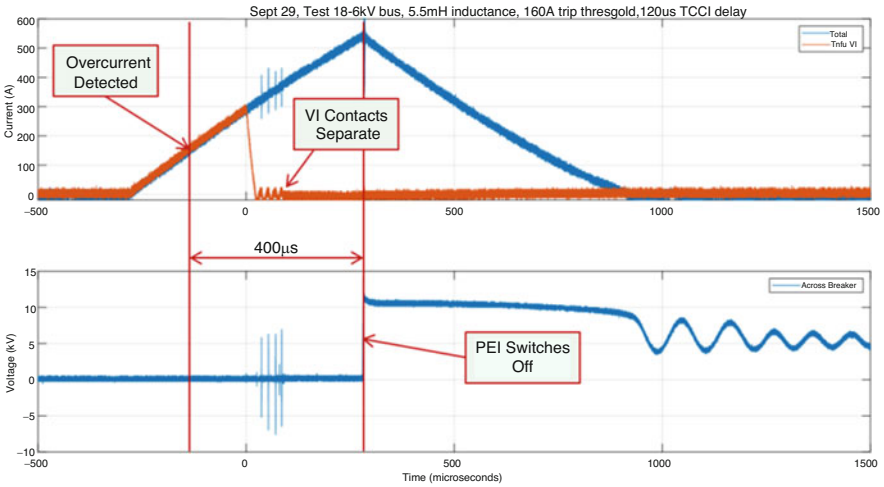

Fig. 11.13 Experimental testing waveforms of HCB fault interruption

spools of wound wire. The test setup and breaker were remotely operated from a separate control room via fiber-optic communications/control link.

Results of the medium voltage met or exceeded the targeted goals, which were to prove the TCCI-based hybrid circuit breaker concept would work at the full 6-kV rated voltage at peak fault current levels equivalent to those achieved in the previous low-current testing rounds. Figure 11.13 illustrates an example trial showing the breaker's ability to interrupt a 6-kV fault within 400 μs after detection with a peak fault current nearly 540 A. As can be seen in the figure, with overcurrent detection threshold set to 160 A, the TCCI activation is delayed 120 μs before it begins commutation of current from the HSVS to the PEI. Once active, the TCCI regulates the HSVS current to a triangular waveform between approximately + and − 12 A.

Once the HSVS vacuum interrupter (VI) contacts begin to separate approximately 220 μs after fault detection, current through the HSVS is halted and remains zero thereafter. At 400 μs after detection, with the HSVS contact gap now at a distance capable of holding off a 12-kV MOV clamping voltage transient, all nine stages of the PEI are simultaneously turned off, thus completing interruption of the circuit. After the energy stored in the inductor is depleted and the fault current falls to zero, the voltage across the breaker settles to the 6-kV source voltage after a short period of oscillations due to the resonance between the line inductance and the PEI snubber capacitance. This test sequence proved the viability of the HCB's operating principle and exceeded the initial test goals.

6 Concluding Remarks

A prototype circuit breaker capable of protecting medium-voltage DC power systems rated up to 6 kV and 200 A was developed. The breaker's design incorporated a unique hybrid architecture employing a novel means of commutating current between mechanical and power electronic conduction paths in breaker. A transient commutation current injector (TCCI) actively drives the current through the mechanical vacuum switch to nearly zero, allowing the vacuum switch to stop current flow without the current zero crossings inherent in AC systems. Since architecturally the TCCI resides outside the steady-state conduction path for the breaker, efficiency of the breaker exceeds what was previously possible in other medium-voltage DC-capable designs.

The performance design goals of this project were based on a notional concept, loosely aligned with requirements for an MVDC shipboard application for the US Navy. Currently, however, there are no true commercial or military applications that precisely match the current ratings of this prototype design, so no plans are in place yet to industrialize it. Nevertheless, the project succeeded in demonstrating that a hybrid circuit breaker based on this novel architecture is indeed a practical approach and could serve as an enabler for the deployment of MVDC systems in a variety of markets (e.g., utility distribution, shipboard power, electric rail, data centers, offshore wind and oil platforms, MV photovoltaic power, fast electric vehicle charging, aerospace, etc.). At the time of this writing, analysis is underway to assess the scalability of this approach for higher voltage and current ratings. Indications at this time are that most MVDC systems will require circuit breaker protection current ratings of 2000–4000 A based on very early-stage system concepts and by drawing analogies from legacy AC systems. It is the team's aspiration that this hybrid approach could be scaled to be compatible with system voltages up to 50 kV or more through multistage series configurations. Understandably, to realize such designs, more research will be required to assess the design trade-offs, including evaluation of available and new power semiconductor devices, sensing technology, capacitive storage elements, high-power density inductive current limiting, and optimization of vacuum interrupters for this higher-voltage range. As an example,

one potential enabler for this could be leveraging wide-bandgap semiconductors capable of voltage ratings beyond what silicon can achieve. This could reduce the number of devices needed in series to implement the power electronic interrupter subsystem.

In order to make MVDC systems a reality, work still remains to study the value propositions MVDC can provide in all the potential markets. Benefits in terms of ROI, efficiency gains, system reliability, and utilization of existing infrastructure need to be quantified through modeling and eventual deployment of pilot project hardware installations. One of the primary objectives of this project was for the development of the prototype to serve as a linchpin for the further evolution of MVDC, filling a long-standing gap, namely, the unavailability of capable protection devices. It is our hope that market entities interested in launching new MVDC systems will recognize this new technology and ultimately utilize it to take the next steps toward fruition.

Acknowledgments The authors of this chapter would like to thank all the project team members who contributed to and participated in this research project to develop the hybrid circuit breaker. This includes Yuanfeng Zhou, Nikolay Shatalov, Risha Na, Tristan Cooper, and Ian Brown of the Illinois Institute of Technology, Jian Liu, Lakshmi Ravi and Rolando Burgos of the Virginia Polytechnic Institute and State University, and Tyler Holp, Xin Zhou, Wangpei Li, Eric Smith, Brad Leccia, Michael Slepian, Brian Carlson, Andy Schroedermeier, Hongbin Wang, Sean Cunningham, Andrew Youel, Antonio Trujillo, and Andrew Rockhill, all with Eaton Corporation. In addition, recognition goes to Richard Byron Beddingfield, Mark Nations and Subhashish Bhattacharya of North Carolina State University, and Paul Ohodnicki of the University of Pittsburgh (via the National Energy Research Laboratory). Furthermore, the authors also extend their gratitude to Isik C. Kizilyalli, Danny Cunningham, Kathleen Lentijo, and Ziaur Rahman of the Advanced Research Projects Agency-Energy of the US Department of Energy for their oversight of and guidance throughout the development of the hybrid circuit breaker.

The information, data, or work presented in this chapter was funded in part by the Advanced Research Projects Agency-Energy (ARPA-E), US Department of Energy, under Award Number DE-AR0001111. The views and opinions of authors expressed herein do not necessarily state or reflect those of the US Government or any agency thereof.

References

1. A. Shukla, G.D. Demetriades, A survey on hybrid circuit-breaker topologies. IEEE Trans. Power Deliv. **30**(2), 627–641 (2015)
2. W. Wen, Y. Huang, Y. Sun, J. Wu, M. Al-Dweikat, W. Liu, Research on current commutation measures for hybrid DC circuit breakers. IEEE Trans. Power Deliv. **31**(4), 1456–1463 (2016)
3. M. Callavik, The hybrid circuit breaker: An innovation breakthrough enabling reliable HVDC grids (2012) [Online], www.abb.com
4. J. Häfner, B. Jacobson, Proactive hybrid HVDC breakers—A key innovation for reliable HVDC grids, in Proceedings of CIGRE Bologna, Italy, 2011
5. R. Derakhshanfar, T.U. Jonsson, U. Steiger, M. Habert, Hybrid HVDC breaker—Technology and applications in point-to-point connections and DC grids, in Proceedings of CIGRE, 2014
6. W. Grieshaber et al., Development and test of a 120kV direct current circuit breaker, in Proceedings of CIGRE, 2014

7. A. Hassanpoor et al., Technical assessment of load commutation switch in hybrid HVDC breaker. IEEE Trans. Power Electron. **30**(10), 5393–5400 (2015)
8. Y. Zhou, Y. Feng, N. Shatalov, Z. John Shen, An ultra-efficient DC hybrid circuit breaker architecture based on transient commutation current injection, in Proceedings of the 35th Annual IEEE Applied Power Electronics Conference (APEC), 2020
9. Y. Zhou, Y. Feng, N. Shatalov, R. Na, Z.J. Shen, An ultraefficient DC hybrid circuit breaker architecture based on transient commutation current injection. IEEE J. Emerg. Sel. Top. Power Electron. **9**(3), 2500–2509 (2021)
10. BREAKERS, Building reliable electronics to achieve kilovolt effective ratings safely (2018), https://arpa-e.energy.gov/technologies/programs/breakers
11. C. Yamazaki, E. Ikawa, I. Tominaga, T. Saito, I. Uchiki, Y. Takami, S. Yamada, Development of a high-precision power supply for bending electromagnets of a heavy ion medical accelerator, in Proceedings of IEEE 8th International Conference on Power Electronics, Asia, May 2011, pp. 3013–3016
12. E. Penovi, R.G. Retegui, S. Maestri, G.U.M. Benedetti, Multistructure power converter with H-bridge series regulator suitable for high-current high-precision-pulsed current source. IEEE Trans. Power Electron. **30**(12), 6534–6542 (2015)
13. P.G. Slade, *The Vacuum Interrupter* (CRC Press, 2008)
14. Cedrat Technologies S.A., "Mechatronic Solutions", 2018
15. B. Lequesne, T. Holp, S. Schmalz, M. Slepian, H. Wang, Frequency-domain analysis and design of Thomson-coil actuators, in 2021 IEEE Energy Conversion Congress and Exposition (ECCE), 2021, pp. 4081–4088
16. ACE, *Damping Technology* (Main Catalog, 2018)
17. IEC, *IEC 60060-1: High-Voltage Test Techniques – Part 1: General Definitions and Test Requirements*, 3rd edn. (International Electrotechnical Commission (IEC), 2010)
18. J. Liu, L. Ravi, D. Dong, R. Burgos, A single passive gate-driver for series-connected power devices in DC circuit breaker applications. IEEE Trans. Power Electron. **36**(10), 11031–11035 (2021)
19. X. Lin, L. Ravi, Y. Zhang, R. Burgos, D. Dong, Analysis of voltage sharing of series-connected SiC MOSFETs and body-diodes. IEEE Trans. Power Electron. **36**(7), 7612–7624 (2021)
20. X. Zhang, Z. Yu, Z. Chen, Y. Huang, B. Zhao, R. Zeng, Modular design methodology of DC breaker based on discrete metal oxide varistors with series power electronic devices for HVdc application. IEEE Trans. Ind. Electron. **66**(10), 7653–7662 (2019)
21. X. Zhang et al., A state-of-the-art 500-kV hybrid circuit breaker for a dc grid: The world's largest capacity high-voltage dc circuit breaker. IEEE Ind. Electron. Mag. **14**(2), 15–27 (2020)
22. R. Rodrigues, Y. Du, A. Antoniazzi, P. Cairoli, A review of solid-state circuit breakers. IEEE Trans. Power Electron. **36**(1), 364–377 (2021)
23. A. Giannakis, D. Peftitsis, Performance evaluation and limitations of overvoltage suppression circuits for low- and medium-voltage DC solid-state breakers. IEEE Open J. Power Electron. **2**, 277–289 (2021)
24. L. Ravi, D. Zhang, D. Qin, Z. Zhang, Y. Xu, D. Dong, Electronic MOV-based voltage clamping circuit for DC solid-state circuit breaker applications. IEEE Trans. Power Electron. **37**(7), 7561–7565 (2022)
25. I. Kim, T. Funabashi, H. Sasaki, T. Hagiwara, M. Kobayashi, Study of ZnO arrester model for steep front wave. IEEE Trans. Power Deliv. **11**(2), 834–841 (1996)
26. C. Xu et al., Piezoelectrically actuated fast mechanical switch for MVDC protection. IEEE Trans. Power Deliv. **36**(5), 2955–2964 (2021)
27. N. Yan, D. Dong, R. Burgos, A multichannel high-frequency current link based isolated auxiliary power supply for medium-voltage applications. IEEE Trans. Power Electron. **37**(1), 674–686 (2022). https://doi.org/10.1109/TPEL.2021.3102055
28. L. Mackey, C. Peng, I. Husain, Progressive switching of hybrid DC circuit breakers for faster fault isolation, in 2018 IEEE Energy Conversion Congress and Exposition (ECCE), 2018, pp. 7150–7157